AD-A188 076 ION ENERGY DIAGNOSTICS FOR VOLTAGE DETERMINATIONS IN PLASMA-EROSION-OPENING-SWITCH EXPERIMENTS(U) NAVAL RESEARCH LAB WASHINGTON DC F C YOUNG ET AL. 03 DEC 87 1/1

UNCLASSIFIED NRL-MR-6059 F/G 20/9 NL

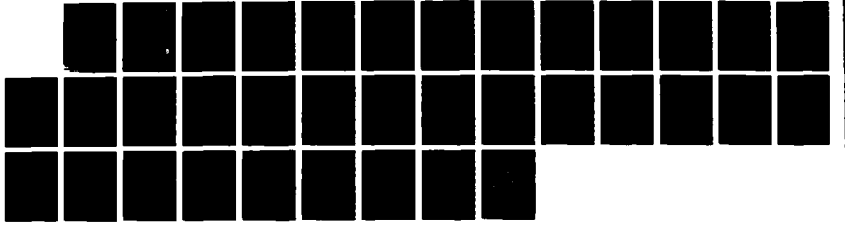

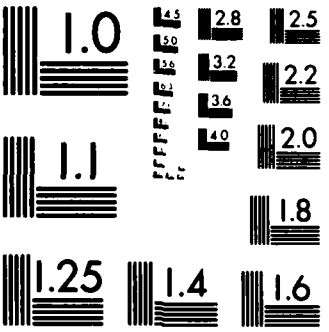

Naval Research Laboratory
Washington, DC 20375-5000

NRL Memorandum Report 6059

Ion Energy Diagnostics for Voltage Determinations in Plasma-Erosion-Opening-Switch Experiments

F.C. YOUNG, J.M. NERI, B.V. WEBER,* R.J. COMMISSO,
S.J. STEPHANAKIS AND T.J. RENK†

Plasma Technology Branch
Plasma Physics Division

**Jaycor, Vienna, VA 22180*

†*NRC Research Associate*

December 3, 1987

SECURITY CLASSIFICATION OF THIS PAGE

REPORT DOCUMENTATION PAGE

Form Approved
OMB No 0704 0188

1a REPORT SECURITY CLASSIFICATION UNCLASSIFIED	1b RESTRICTIVE MARKINGS
2a SECURITY CLASSIFICATION AUTHORITY	3 DISTRIBUTION/AVAILABILITY OF REPORT Approved for public release; distribution unlimited.
2b DECLASSIFICATION/DOWNGRADING SCHEDULE	
4 PERFORMING ORGANIZATION REPORT NUMBER(S) NRL Memorandum Report 6059	5 MONITORING ORGANIZATION REPORT NUMBER(S)
6a NAME OF PERFORMING ORGANIZATION Naval Research Laboratory 6b OFFICE SYMBOL (If applicable) Code 4770	7a NAME OF MONITORING ORGANIZATION
6c ADDRESS (City, State, and ZIP Code) Washington, DC 20375-5000	7b ADDRESS (City, State, and ZIP Code)
8a NAME OF FUNDING/SPONSORING ORGANIZATION Department of Energy 8b OFFICE SYMBOL (If applicable)	9 PROCUREMENT INSTRUMENT IDENTIFICATION NUMBER
8c ADDRESS (City, State, and ZIP Code) Washington, DC 20545	10 SOURCE OF FUNDING NUMBERS PROGRAM ELEMENT NO: DOE PROJECT NO: NONE TASK NO: DE-AI08 79DP40092 WORK UNIT ACCESSION NO: DN680-382

11 TITLE (Include Security Classification)
Ion Energy Diagnostics for Voltage Determinations in Plasma-Erosion-Opening-Switch Experiments

12 PERSONAL AUTHOR(S)
Young, F.C., Neri, J.M., Weber,* B.V. Commisso, R.J., Stephanakis, S.J., Renk,+ T.J.

13a TYPE OF REPORT	13b TIME COVERED	14 DATE OF REPORT (Year, Month, Day)	15 PAGE COUNT
Interim	FROM 7/83 TO 7/86	1987 December 3	35

16 SUPPLEMENTARY NOTATION
*JAYCOR, Vienna, VA 22180
+NRC Research Associate,

17 COSATI CODES		
FIELD	GROUP	SUB-GROUP

18 SUBJECT TERMS (Continue on reverse if necessary and identify by block number)
Pulsed power; Neutron time-of-flight; Plasma erosion-opening-switch; Ion-beam activation; Ion-diode voltage; Stacked-foil activation

19 ABSTRACT (Continue on reverse if necessary and identify by block number)

A number of nuclear techniques have been developed and used to measure ion-diode voltages for plasma-erosion-opening-switch (PEOS) experiments on the Gamble II pulsed-power generator at NRL. The voltage is determined by measuring the energy of protons or deuterons from the diode. The techniques include neutron time-of-flight, neutron-intensity measurements, delayed activations, and stacked-foil activations. These diagnostics have evolved as the voltage developed in PEOS experiments have increased from less than 1 MV to more than 4 MV. Examples of these diagnostics are presented, and the extension of some of these techniques to voltages of more than 20 MV is described.

20 DISTRIBUTION/AVAILABILITY OF ABSTRACT [X] UNCLASSIFIED/UNLIMITED [ ] SAME AS RPT [ ] DTIC USERS	21 ABSTRACT SECURITY CLASSIFICATION UNCLASSIFIED
22a NAME OF RESPONSIBLE INDIVIDUAL F.C. Young	22b TELEPHONE (Include Area Code) (202) 767-2610 22c OFFICE SYMBOL Code 4770

DD Form 1473, JUN 86 *Previous editions are obsolete* SECURITY CLASSIFICATION OF THIS PAGE

S/N 0102-LF-014-6603

CONTENTS

ION ENERGY DIAGNOSTICS FOR VOLTAGE DETERMINATIONS IN PLASMA-EROSION-OPENING-SWITCH EXPERIMENTS

I. INTRODUCTION

The use of a plasma erosion opening switch (PEOS) in inductive-store pulsed-power systems may result in diode load voltages of several megavolts.[1,2] Voltages exceeding 4 MV have been achieved in experiments[2] with a PEOS at the Naval Research Laboratory (NRL), and voltages approaching 30 MV are required for the PBFAII, light-ion-beam, inertial-confinement-fusion driver at Sandia National Laboratories.[3]

The load voltage in pulsed-power experiments is usually determined by making inductive corrections using current and voltage probes, which, of necessity, are located at some distance from the load. The experimental arrangement for a vacuum inductive store with a PEOS is shown in Fig. 1 for the Gamble II generator at NRL. To determine the load voltage, V_L, from electrical measurements, the upstream current, I_u, and the load or downstream current, I_L, must be measured and used to inductively correct the insulator voltage, V_d, according to

$$V_L = V_d - L_I(dI_u/dt) - L(dI_L/dt). \qquad (1)$$

For this Gamble II configuration, the load inductance, $L \approx 10\text{-}20$ nH, is much smaller than the store inductance, $L_I \approx 100\text{-}130$ nH. Then, the load voltage is given approximately by the switch voltage, V_{sw}, where

$$V_{sw} = V_d - L_I(dI_u/dt). \qquad (2)$$

It is difficult to evaluate the load voltage using Eq. 1 or Eq. 2 because the inductive corrections may be inaccurate for any or all of the

Manuscript approved September 28, 1987.

following reasons. Voltage multiplication in the inductive store region may cause the vacuum insulator to flashover. Time-varying current paths in the switch plasma may represent unknown time-dependent inductances. For finite impedance loads, current losses may occur between the switch region and the load. Finally, this inductive correction relies on taking the difference between two comparable electrical measurements which often have poor signal-to-noise ratios and may be perturbed by the intense electromagnetic and radiation environment.

Nuclear techniques can be used to measure the maximum load voltage for ion-diode loads in a way that is non-perturbing to the load and is insensitive to the noisy electrical environment. A measurement of the energy of protons or deuterons produced in an ion diode provides a direct measure of the diode voltage because for singly charged ions, the load voltage is the ion energy divided by the electronic charge. The yields of nuclear reactions are particularly attractive for multi-MeV ion energies, and a nuclear measurement can be used to determine the voltage at the load without perturbing the load. The techniques described here have the disadvantage that they do not provide time resolved voltage but only determine a maximum or average value. Four different nuclear techniques for determining load voltages are presented in this report: 1) neutron time-of-flight (TOF), 2) absolute neutron-intensity measurements, 3) delayed activations, and 4) stacked-foil activations. Each of these techniques will be described, and results from applying these techniques to PBFA experiments will be presented.

II. NEUTRON TIME-OF-FLIGHT

If the generator is operated with positive voltage on the center conductor so that ions from an ion diode are directed away from the generator, then the energy of forward-emitted neutrons can be measured with

a TOF detector located several meters from the target. The ion energy is determined from the measured neutron energy using reaction kinetics as shown in Fig. 2 for two different nuclear reactions. Forward-emitted neutrons are used to optimize the sensitivity of the ion energy to the neutron energy. The neutrons must have sufficient energy and the reaction cross section must be large enough to produce a measurable pulse of neutrons in a scintillator-photomultiplier detector. Our experience leads us to recommend the $^{2}H(d,n)$ reaction for deuterons with energies > 0.5 MeV and the $^{7}Li(p,n)$ reaction for protons with energies > 3 MeV. The cross sections for both of these reaction have been measured extensively, and the reaction kinematics are well documented.[4,5] The cross sections of both reactions are strongly forward peaked.

There is an intense bremsstrahlung pulse associated ith a pulsed-power driven ion diode which provides a timing reference for when neutrons are emitted from the diode. It is assumed that the neutrons and the x rays originate simultaneously at the diode during the power pulse. The neutron flight path should be adjusted so that the neutron pulse occurs well after the bremsstrahlung pulse. This allows the TOF detector to recover from the bremstrahlung pulse and record the neutron pulse. The longer the flight path and flight time, the more precisely the neutron energy is determined. Of course, the detector must be located sufficiently close to the source so that the neutron pulse can be detected above the background level of the detector. The thickness of the targets used is much less than the ion range so that the temporal dispersion of the neutron pulse due to ion energy loss in the target is minimized.

Neutron TOF measurements with the $^{2}H(d,n)$ reaction for PBFA experiments on the Gamble II generator are shown in Fig. 3. The center conductor polarity was positive, and a pinched-beam ion diode with an anode coated with deuterated

polyethylene (CD_2) was used to produce a deuteron beam. (The locations of the anode and cathode are interchanged from those shown in Fig. 1.) Deuterons were accelerated across the anode-cathode gap and bombarded a CD_2 target located on the cathode to produce an intense pulsed neutron source. The TOF detector was located 7 m from the CD_2 target along the axis of the generator. For neutron energies < 6 MeV and a 7-m flight path, the flight time is > 200 ns, and neutrons arrive at the detector well after the 50-ns duration x-ray pulse from the diode. The scintillator-photomultiplier TOF detector was embedded in a 3.2-cm thick lead shield to attenuate the bremsstrahlung. Even so, the x-ray pulse saturated the detector output at ≈ 40 V, as shown in Fig. 3.

Two different methods were used to evaluate the neutron energy from these TOF measurements. For method 1, the neutron and x-ray pulses were measured on a slow sweep (50 ns/div.), and the interval between the 50% risetime points on these pulses was measured; this corresponds to the 4.1-MeV neutron energy in Fig. 3. For this case, the x-ray pulse was saturated, and its peak is not well defined. For method 2, the neutron trace was measured on a fast sweep (20 ns/div.), and the x-ray pulse (unsaturated) was measured with a scintillator-photodiode detector. The time interval between the peaks of these signals from two different detectors was determined. This interval corresponds to the 3.8-MeV neutron energy in Fig. 3. This neutron energy implies a deuteron energy of 0.7 MeV. For higher deuteron energies of 2 to 3 MeV, the neutron signal would occur earlier in time as indicated at the bottom of Fig. 3. For both methods, appropriate corrections were made for x-ray flight times from the diode to the detectors, for delay in the TOF photomultiplier detector, and for the deuteron flight time from the anode to the CD_2 target.

Deuteron energies determined by these two methods for four different shots are compared in Table I. The larger uncertainties for method 1 result from the slower sweep time and less precise timing. The energies obtained

Table I

Deuteron Energy Measurements by Neutron Time-of-Flight

Shot No.	Deuteron Energy (MeV)	
	Method 1	Method 2
2507	0.6 ± 0.2	0.8 ± 0.15
2509	0.9 ± 0.3	0.84 ± 0.15
2511	0.84 ± 0.25	0.75 ± 0.15
2513	1.0 ± 0.3	0.7 ± 0.1

with these two methods are in agreement. Comparison of the upstream and downstream currents in Fig. 3 indicates slower-than-optimum switch opening and significant current losses. These low deuteron energies are attributed to the combination of large diameter conductors in the switch region and positive-polarity operation.[6]

For experiments where the PEOS operation produced voltages exceeding 3 MV on the diode,[7] neutron TOF measurements were unsuccessful. At these higher voltages, the bremsstrahlung was so intense that the TOF detector was unable to recover from the x-ray pulse in time to record the neutron pulse. For these measurements, the detector was located within a shielded room surrounding the diode. If the detector were located outside this room and at a larger neutron flight path so that direct line-of-sight from the detector is restricted to just the neutron source, it is likely that this detector recovery problem could be overcome. This detector geometry has been used successfully on Gamble II to make neutron TOF measurements from exploded CD_2 fibers.[8] In this case, the TOF detector was located ≈ 10 m outside the shielded room at 68° to the diode axis. For ion-diode experiments on the Gamble II generator, it was not possible to increase the neutron flight path in the forward direction to more than ≈ 7 m.

Neutron TOF measurements with the ^7Li p,n ^7Be reaction have been carried out on a higher voltage pulsed-power generator.[9] This reaction is attractive

for this application because even at the higher voltages, the neutron velocities are small enough so that the neutrons can be adequately delayed relative to the bremsstrahlung for reasonable flight paths. For the experiment in Ref. 9, the TOF detector was located 13.8 m from a LiCl target and at 10° to the generator axis. The detector was embedded in a 5.1-cm thick lead shield to attenuate the bremsstrahlung from the diode, and thick LiCl targets were used to increase the neutron output. Detector traces for shots with and without a target are compared in Fig. 4. In this experiment, the duration of proton emission from the diode and the neutron energy dispersion from protons stopping in the thick LiCl target are primary contributors to the width of the neutron pulse. An average proton energy of 4.3 MeV is determined from the time interval from the peak of the x-ray pulse to the peak of the neutron pulse. A maximum proton energy of 5.4 MeV is based on measuring from the 50% point on the leading edge of the neutron pulse.

In summary, the ion diode load voltage can be measured by neutron time-of-flight for sufficiently long flight paths. Forward-emitted neutrons must be detected for optimum sensitivity which may require positive polarity operation of the pulsed-power generator so that these neutrons are directed away from the generator. The $^{2}H(d,n)$ reaction is appropriate for energies > 0.5 MeV, and the $^{7}Li(p,n)$ reaction is appropriate for energies > 3 MeV. This technique does not require a measurement of the ion current. The challenge with this diagnostic is to shield the TOF detector adequately from the intense prompt bremsstrahlung pulse so that the delayed neutron pulse can be measured.

III. NEUTRON INTENSITY MEASUREMENTS

For proton energies greater than 1.9 MeV, the yield of neutrons from the $^7Li(p,n)$ reaction is a sensitive function of the proton energy, and a measurement of the number of neutrons can be used to determine the proton energy and thus estimate the diode voltage. Figure 5 presents the thick-target yield for the $^7Li(p,n)$ reaction on a LiCl target for neutrons emitted at 15° to the incident proton beam; conditions corresponding to measurements on the Gamble II generator. This yield was evaluated from tabulated reaction cross sections,[4] σ, and proton stopping cross sections,[10] ϵ, according to

$$Y(E) = \int(\sigma/\epsilon)de \qquad (3)$$

where the integration is from the threshold energy to the incident proton energy, E. This thick-target yield increases rapidly with proton energy from a threshold at 1.88 MeV so that a measurement of the neutron intensity can be used to infer the energy of protons from 1.9 to more than 4.5 MeV.

To relate the thick-target yield to the measured number of neutrons, the ion current on target and the pulse shape for the diode-load voltage are required. The ion current on the LiCl target was measured with a Rogowski current monitor as shown in Fig. 1. The switch voltage, determined from Eq. 2, was used for the voltage pulse shape. Then the number of neutrons/sr, N_n, is given by

$$N_n = \int I(t)\cdot Y[E(t)]dt \qquad (4)$$

where the shape of E(t) is given by the switch voltage, $V_{sw}(t)$. The energy, E(t), is scaled from $V_{sw}(t)$ to fit the measured number of neutrons so that

$$E(t) = F\cdot V_{sw}(t) \qquad (5)$$

where F is a scale factor.

For experiments on Gamble II, the number of neutrons was measured with a Mn-Cu activation detector which had been calibrated absolutely for neutrons from the $^{7}Li(p,n)$ reaction.[11] The detector consisted of a Mn-Cu foil (2.5-cm dia by 25-μm thick) embedded in a 7.6-cm dia by 7.6-cm thick polyethylene moderator. Neutrons, moderated in the polyethylene, induced activity in the embedded foil by the $^{55}Mn(n,\gamma)^{56}Mn$ reaction. For Gamble II operated in negative polarity, the proton beam was directed toward the generator. A pinched-beam diode with a polyethylene anode was used to produce the proton beam, and the signal from the ion-current Rogowski on the center conductor (see Fig. 1) was recorded through a transit-time isolator. To measure the forward-emitted neutrons from the $^{7}Li(p,n)$ reaction, the compact Mn-Cu detector was located within the center conductor of the generator. After a shot, there was sufficient time to remove the Mn-Cu foil and measure the 156-min ^{56}Mn activity.

The results of four PEOS shots on Gamble II operated in negative polarity are presented in Table II. The measured ion-current and switch-voltage traces for these four shots are given in Fig. 6. For shot 2715, a smaller anode-cathode gap was used, and no neutrons were detected. For this lower-impedance diode condition, the proton energy did not exceed the 1.9-MeV threshold energy; a result consistent with the switch-voltage trace.

Table II

Proton Energies from Neutron-Intensity Measurements

Shot No.	A-K Gap (mm)	N_n (10^{10} neut/sr)	F	Max. Energy (MeV)
2714	11	1.55 ± 0.10	0.81	2.4
2715	5	<0.15	-	-
2716	11	1.33 ± 0.15	0.76	2.6
2717	11	0.22 ± 0.05	0.61	2.2

For the other three shots, the current and voltage traces shown in Fig. 6 were used to calculate neutron intensities according to Eq. 4. In all three cases, the calculated intensity was larger than the measured intensity so the switch voltage was scaled according to Eq. 5 to fit the measured intensity. The scale factors and the maximum ion energies required to reproduce the measured neutron intensities are given in Table II. The scale factor is a sensitive function of the neutron intensity as shown in Fig. 7 for shot 2714. To the extent that the measured ion currents are not 100% protons, the energies in Table II represent lower limits on the diode voltage.

These neutron intensity measurements indicate that diode voltages of at least 2.6 MV are produced in negative-polarity PEOS experiments on Gamble II. These voltages are higher than the results presented in Section II due to improved PEOS performance in negative polarity

In summary, neutron intensity measurements with the $^{7}Li(p,n)$ reaction can be used to infer ion-diode voltages in excess of 2 MV. Measurements can be made for proton beams directed toward a pulsed-power generator by using a compact neutron detector located inside the generator. However, this diagnostic requires independent measurements of the ion current on the neutron-producing target and of the waveshape of the load voltage.

IV. DELAYED ACTIVATIONS

For protons with energies greater than 3 MeV, a variety of (p,n) nuclear reactions which produce delayed positron radioactivity can be used to infer the proton energy and the diode voltage. In general, (p,n) reactions on different target nuclei have different threshold energies and cross sections. Some of these reactions are attractive for this application because they have rapidly increasing cross sections just above the threshold energy so their

thick-target yields are sensitive functions of the proton energy. Five suggested (p,n) reactions with threshold energies ranging from 3 MeV to more than 7 MeV are listed in Table III. These reactions were selected for the following reasons: (1) The large isotopic abundances, large cross sections, and large positron decay branchings optimize the activities relative to competing activities induced by naturally occurring deuterons in the ion beam. (2) The single-element targets are readily available, and the half-lives are convenient for counting after pulsed activation. (3) The positron activity can be measured efficiently by coincidence counting.[12] Small beam intensities (> 10^{10} protons) are acceptable, and the beam current density on target must be small (< few kA/cm^2) to avoid loss of radioactivity by target ablation.

Cross sections[13] for these five reactions are displayed in Fig. 8. In all cases, the cross sections increase rapidly from threshold to values of several hundred mbarns. Simultaneous measurements with several of these targets can provide limits on the proton energy. For example, if these five targets are exposed to the same proton beam, and the B, Ti and Cu targets are activated but the Mn and Ni targets are not activated, then the proton energy must be between 4.2 MeV and 5.9 MeV. In this way, the maximum energy

Table III

(p,n) Threshold Reactions to Produce β^+ Activities

Threshold Energy (MeV)	Target Nucleus	Isotopic Abundance (%)	Residual Nucleus	Half-Life (min)	β^+ Decay (%)
3.02	^{11}B	80	^{11}C	20	100
3.77	^{47}Ti	7.5	^{47}V	31	96
4.21	^{63}Cu	69	^{63}Zn	38	80
5.90	^{52}Cr	84	^{52m}Mn	21	92
7.17	^{60}Ni	26	^{60}Cu	23	58

of a proton beam in the range from 3 MeV to more than 7 MeV can be estimated. To be more quantitative, measured activities can be used as described in the next paragraph.

The ratio of β^+ activities measured for two of these reactions can be used to determine an average proton energy. This procedure is illustrated in Fig. 9 for the $^{11}B(p,n)$ and $^{63}Cu(p,n)$ reactions. Thick-target yields for these reactions on boron nitride and copper targets, calculated according to Eq. 3, are displayed in this figure along with the ratio of the number of radioactive nuclei produced by these two reactions. In the region from 4.2 to 6 MeV, this ratio is a sensitive function of the proton energy. Measurements of this ratio with ± 10% precision determine the proton energy to ± 300 keV at 6 MeV and to even smaller uncertainty at lower energy. Only the relative activity of each sample is required, not the absolute activit , so the measurement is simplified. This technique can be used with other pairs of reactions in Table III to provide similar ratios which are sensitive to the proton energy in higher or lower energy ranges. The energy range of this technique is appropriate for PEOS ion-diode experiments on the Supermite generator (4 MV, 2.2 Ω) at Sandia National Laboratories.

Simultaneous activations with the (p,n) reactions in Table III have not been used to measure ion-diode voltages, but simultaneous deuteron activations with the $^{12}C(d,n)^{13}N$ and $^{27}Al(d,p)^{28}Al$ reactions have been used to determine deuteron energies from pulse-power sources.[8,12] This technique was tried with the PEOS experiments on Gamble II. Side-by-side carbon and aluminum targets were exposed to the deuteron beam from an inverse pinched-beam diode. The beam intensity on target was limited by mounting the 1-cm^2 area targets 6-cm behind a 6.4-mm dia aperature which restricted the ion beam on target. Target activations were measured, but the results

indicated that the beam current was not evenly distributed between the two targets. The ion beam had low divergence, did not spread from the diode, and struck the targets non-uniformly and non-reproducibly. This activation technique requires that an equivalent beam strike each target. A solution to this problem would be to ensure a uniform beam distribution onto both targets by Rutherford scattering the beam through a thin gold foil. Alternatively, a composite target could be used where the carbon and aluminum are homogeneously mixed in known proportion.

In summary, the ratio of delayed activations induced by either proton or deuteron beams can be used to determine diode voltages ranging from ≈ 1 MV to more than 7 MV. For voltages > 3 MV, (p,n) reactions are recommended because they have greater sensitivity to the ion energy than do the deuteron-induced reactions. This technique measures an average ion-beam energy weighted towards high energy by the thick-target yields. A uniform beam distribution on target is required with a current density small enough to avoid target ablation. However, measurement of the ion-beam current is not required.

V. STACKED-FOIL ACTIVATIONS

The delayed-activation technique can be extended to the use of stacked foils to measure the maximum diode voltage. This technique has been used in several laboratories to measure energy spectra of collectively accelerated protons.[14] The $^{63}Cu(p,n)$ reaction has been used in these experiments, but this technique can be used with any of the reactions discussed in Sect. IV. To measure the maximum ion energy, the activity in a stack of thin foils bombarded by the ion beam is determined as a function of the depth into the stack. The range-energy relation is used to convert

the depth in the stack to ion energy. For the (p,n) reactions in Table III, the proton energy must exceed the threshold energy before any activity is produced. Higher energy ions penetrate furthur into the stack and induce activity at greater depth. A determination of the deepest activated foil is sufficient to show that the ion energy is larger than the energy needed to reach that foil and is less than the energy required to activate the next foil. In this case, the energy resolution is limited by the foil thickness.

The energy can be determined with greater precision by using the relative activity between adjacent foils. For a given incident ion energy, the activity in a foil stack decreases rapidly near the threshold energy for the (p,n) reactions or near the end of the range for the deuteron-induced reactions. Consequently, the relative activity of the deepest foils is a sensitive function of the maximum ion energy. To interprete such measurements, a monoenergetic incident beam energy is assumed and the relative activity of adjacent foils is calculated. The ratio of measured activities of adjacent deepest foils is compared with the calculations to determine the incident ion energy. This analysis underestimates the maximum ion energy because lower energy ions can contribute to the activity of the next-to-deepest, but not to the deepest foil. Even so, this technique is still very sensitive to the maximum ion energy.

The stacked-foil technique has been used to measure the maximum deuteron energy or ion-diode voltage for PEOS experiments with an inverse ion diode on the Gamble II generator.[2] The delayed activation of carbon in a stack of six 25-μm thick polyethylene (CH_2) foils was measured as a function of depth in the foil stack. The 10-min ^{13}N activity from the $^{12}C(d,n)^{13}N(\beta^+)^{13}C$ reaction was used for this measurement. The 0.51-MeV annihilation radiation associated with the β^+ decay was measured with a

7.6-cm x 7.6-cm NaI detector and multichannel pulse height analyzer. The initial activities in foils #3 through #6 are shown in Fig. 10 as a function of depth into the stack. Foils #1 and #2 were melted and contaminated with radioactivity from the diode. No measurable activity was induced in foil #6. The relative activity in each CH_2 foil was calculated using the thick-target yield[8] for this reaction and stopping cross sections[10] for deuterons in CH_2. In Fig. 11, the calculated ratios of activities for foil #4/foil #3 and foil #5/foil #3 are compared with the measured ratios with the background subtracted. Both measured ratios are consistent with an incident deuteron energy of 3.65 ± 0.05 MeV. The large voltage multiplication (a factor of 2.4) for this experiment is attributed to the use of smaller diameter conductors in the switch region and to negative-polarity operation.

Ratios of activities for adjacent foils in a CH_2 foil stack are presented in Fig. 12. Activities are produced in the first two foils by 2-MeV deuterons, but the energy must exceed 2.4 MeV or 3.0 MeV to induce activity in the third or fourth foil, respectively. In later experiments[2] on Gamble II, the CH_2 foil stack was covered with a 25-μm thick aluminum foil to shield the stack from carbon activity produced in the diode region. The energy loss in this aluminum covering has been added to the energy onto the CH_2 foil stack to give the deuteron energy from the diode, as shown at the top of Fig. 12. The curves in Fig. 12 demonstrate the sensitivity of the relative activity to the incident deuteron energy. For example, a ± 10% measurement of the relative activity corresponds to ± 50 keV uncertainty in the diode voltage. By using the deepest foils in the stack, this measurement samples the most energetic deuterons from the diode. Lower energy deuterons contribute to the activities of the shallow foils in the stack, and the activities of these foils are not used. This technique may be extended to

higher diode voltages by including more CH_2 foils in the stack, or by using any of the reactions listed in Table III. In addition, the uncertainty in the voltage determination may be reduced by using thinner foils. For example, for the measurements in Ref. 2, 12.7-μm thick CH_2 foils were used, and the maximum deuteron energy was 4.25 ± 0.02 MeV, corresponding to a voltage multiplication of 2.3.

In summary, the delayed activation of stacked foils by protons or deuterons from an ion diode can be used to measure the diode voltage. Voltages exceeding 4 MV have been determined with the $^{12}C(d,n)^{13}N$ reaction by measuring the activities of only a few foils in a CH_2 foil stack. The maximum diode voltage can be determined to ≈ 1% uncertainty with 10 to 20-μm thick foils. The (p,n) reactions in Table III can be used to extend this technique to voltages exceeding 10 MV. At higher energies, the activity induced in the deepest foils is less sensitive to the ion energy due to increased ion straggling near the end of the range. This problem is minimized by using the threshold reactions shown in Fig. 8 where the rapidly varying activity in the foil stack occurs at much higher ion energies. The ratio of activities for adjacent foils in a stack can be calculated as a function of the proton energy for the reactions in Table III, and the maximum energy can be determined by measuring the listed positron activities. If the voltage is known approximately, for example, by delayed activation measurements as described in Sect. IV, then the stacked foil can be designed so that only a few foil activity measurements are needed to determine the voltage.

VI. SUMMARY

Four different nuclear techniques have been developed and used to determine voltages for PEOS experiments on the Gamble II generator. Neutron TOF with $^{2}H(d,n)$ neutrons was used for voltages of ≈ 1 MV, but was not useful at ≈ 3 MV due to intense bremsstrahlung from the diode. This technique has been used successfully at higher voltages with $^{7}Li(p,n)$ neutrons. The intensity of forward-emitted neutrons from the $^{7}Li(p,n)^{7}Be$ reaction was measured to determine voltages larger than 2 MV. This technique was used when the neutrons were directed toward the pulsed-power generator so that neutron TOF measurements were impossible. Delayed activations induced by different (p,n) threshold reactions were recommended for voltages greater than 3 MV. The relative activations produced by two different (p,n) reactions could be used to determine voltages ranging from 3 MV to more than 7 MV. This technique has been demonstrated with deuteron-induced reactions at ≈ 3 MV, but it was not successful for PEOS experiments because the ion-beam was not distributed uniformly on the activation targets. Stacked-foil activations were developed to overcome this difficulty. In PEOS experiments, voltages of ≈ 4 MV have been determined by measuring the ^{13}N activity induced in stacked CH_2 foils by $^{12}C(d,n)$ reactions. Higher voltages, up to more than 10 MV, could be determined by using (p,n) threshold reactions. As intense ion beams of higher voltage are developed, it is expected that these techniques will find greater application.

VII. ACKNOWLEDGEMENTS

The interest and encouragement for this work by R.A. Meger and G. Cooperstein is appreciated. This research was supported by the U. S. Department of Energy.

REFERENCES

1. R.A. Meger, R.J. Commisso, G. Cooperstein, and Shyke A. Goldstein, Appl. Phys. Lett. 42, 943 (1983).
2. J.M. Neri, J.R. Boller, P.F. Ottinger, B.V. Weber and F.C. Young, Appl. Phys. Lett. 50, 1331 (1987).
3. J.P. VanDevender and D.L. Cook, Science 232, 831 (1986).
4. H. Liskien and A. Paulsen, At. Nucl. Data Tables,11,569 (1973).
5. H. Liskien and A. Paulsen, At. Nucl. Data Tables 15, 57 (1975).
6. B.V. Weber, R.J. Commisso, W.F. Oliphant and P.F. Ottinger, abstracts 1984 IEEE Inter. Conf. on Plasma Science, IEEE Publ. No. 84CH1958-8, St. Louis, MO, 1984, p. 8.
7. J.M. Neri, J.R. Boller, R.J. Commisso, R.A. Meger, P.F. Ottinger, T.J. Renk, B. V. Weber and F.C. Young, Abstracts 1985 IELE Inter. Conf. on Plasma Science, IEEE Cat. No. 85CH2199-8, Pittsburg, PA, 1985, p. 55.
8. F.C. Young, S.J. Stephanakis and D. Mosher, J. Appl. Phys. 48, 3642 (1977).
9. R.A. Meger and F.C. Young, J. Appl. Physics 53, 8543 (1982).
10. H.H. Andersen and J.F. Ziegler, The Stopping and Ranges of Ions in Matter (Pergamon, New York, 1977) Vol. 3.
11. F.C. Young and J.G. Pronko, Rev. Sci. Instrum. 53, 1228 (1982).
12. F.C. Young, J. Golden and C.A. Kapetanakos, Rev. Sci. Instrum. 48, 432 (1977).
13. G.F.J. Legge and I.F. Bubb, Nucl. Phys. 26, 616 (1961) for $^{11}B(p,n)$; S. Tanaka and M. Furukawa, J. Phys. Soc. Jpn. 14, 1269 (1959) for $^{47}Ti(p,n)$; J. Wing and J.R. Huizenga, Phys. Rev. 128, 280 (1962), and F. Boehm, P. Marmier and P. Preiswerk, Helv. Phys. Acta. 25, 599 (1952) for $^{52}Cr(p,n)$; J.N. Barrandon, J.L. DeBrun, A. Kohn and R.H. Spear,

Nucl. Instrum. Methods 127, 269 (1975) for $^{60}Ni(p,n)$; R. Colle, R. Kishore and J.B. Cumming, Phys. Rev. C9, 1819 (1974) for $^{63}Cu(p,n)$.

14. R.J. Adler, J.A. Nation and V. Serlin, Rev. Sci. Instrum. 52, 698 (1981).

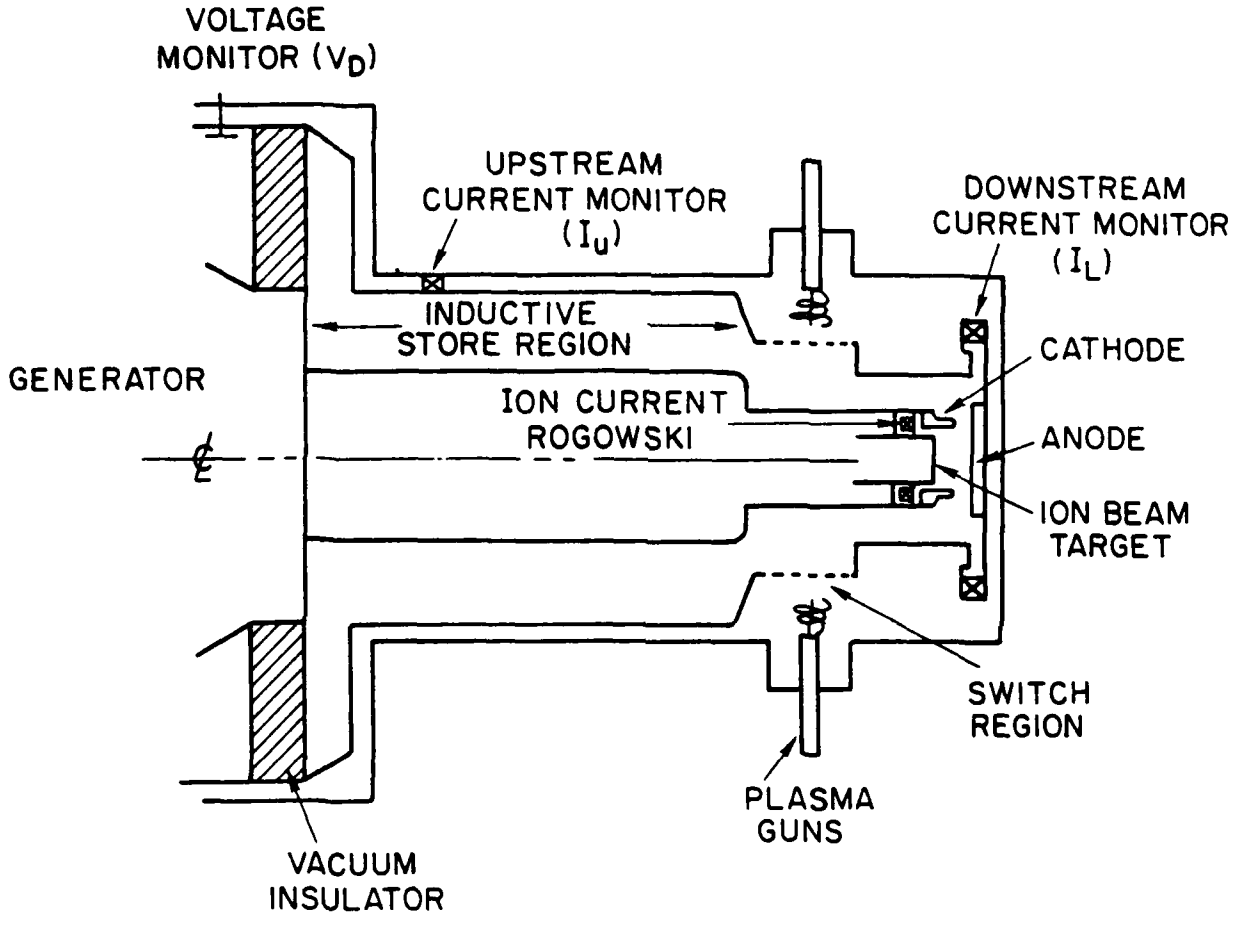

Fig. 1. Experimental arrangement for a vacuum inductive store and plasma erosion opening switch on the Gamble II generator.

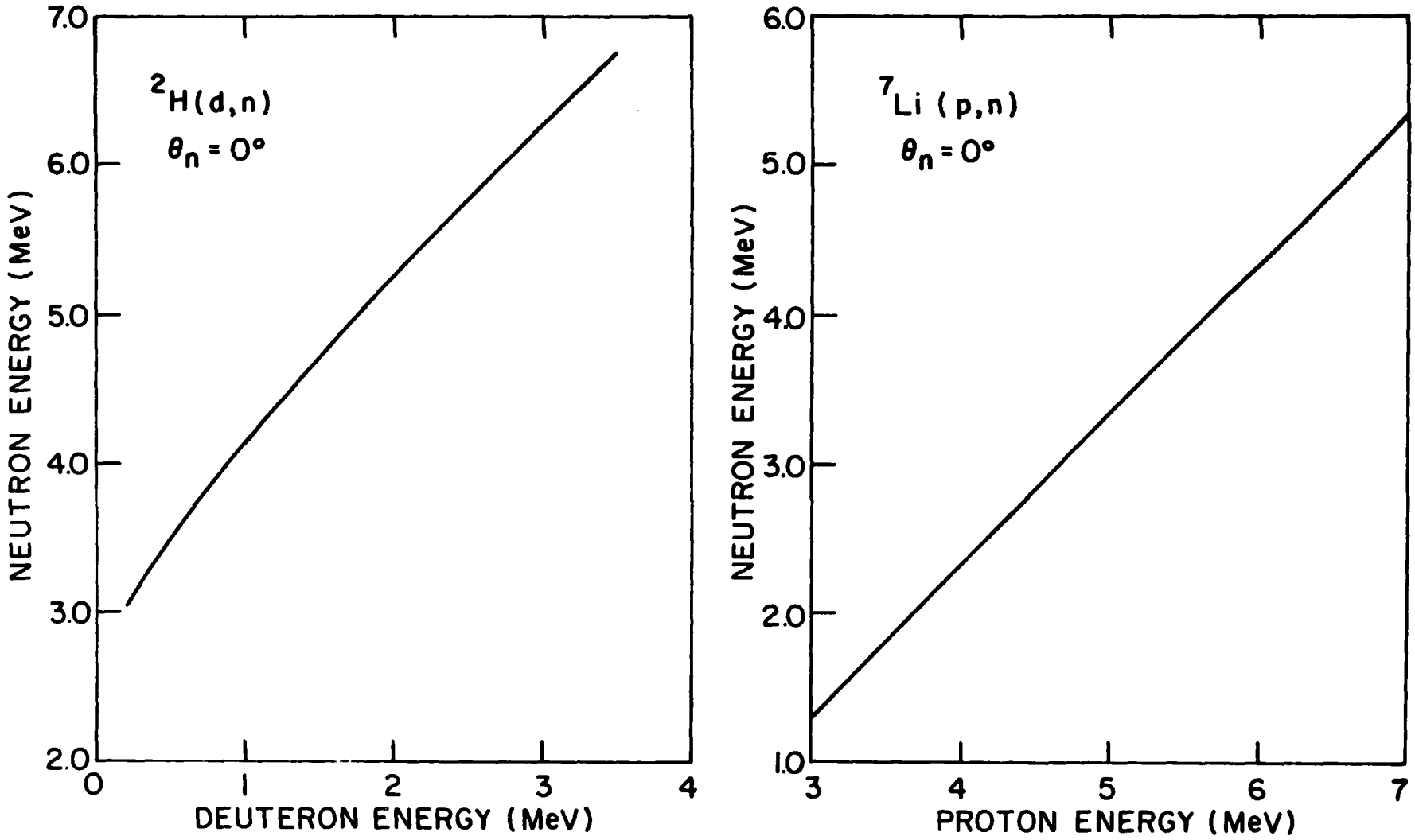

Fig. 2. Kinematic relation between the energy of forward-emitted neutrons and the incident ion energy for the $^2H(d,n)^3He$ and $^7Li(p,n)^7Be$ reactions.

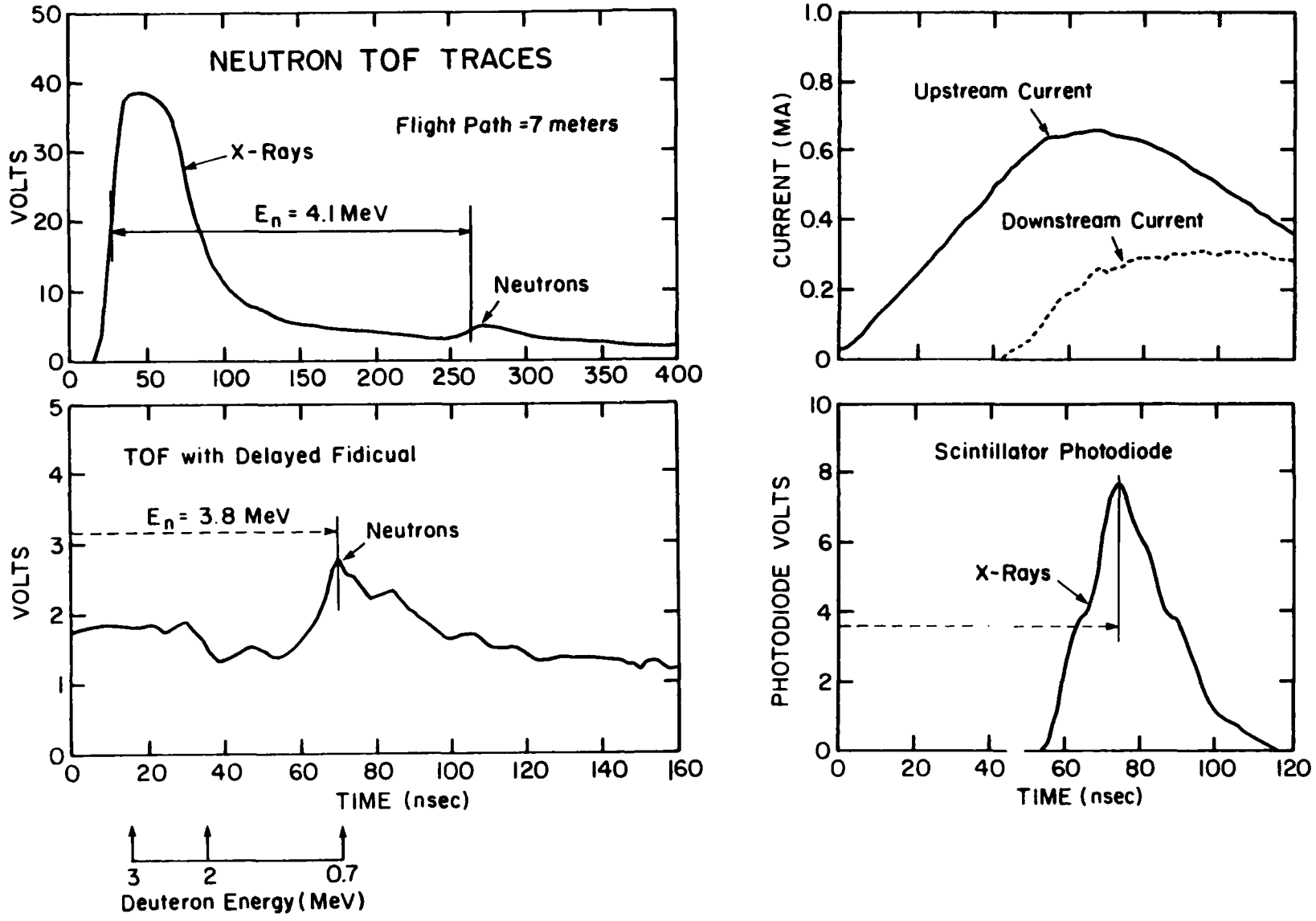

Fig. 3. Experimental traces for a PEOS shot on Gamble II with a neutron TOF detector. The neutron detector trace on the left is recorded on two different time scales. X-ray and current traces are on the right.

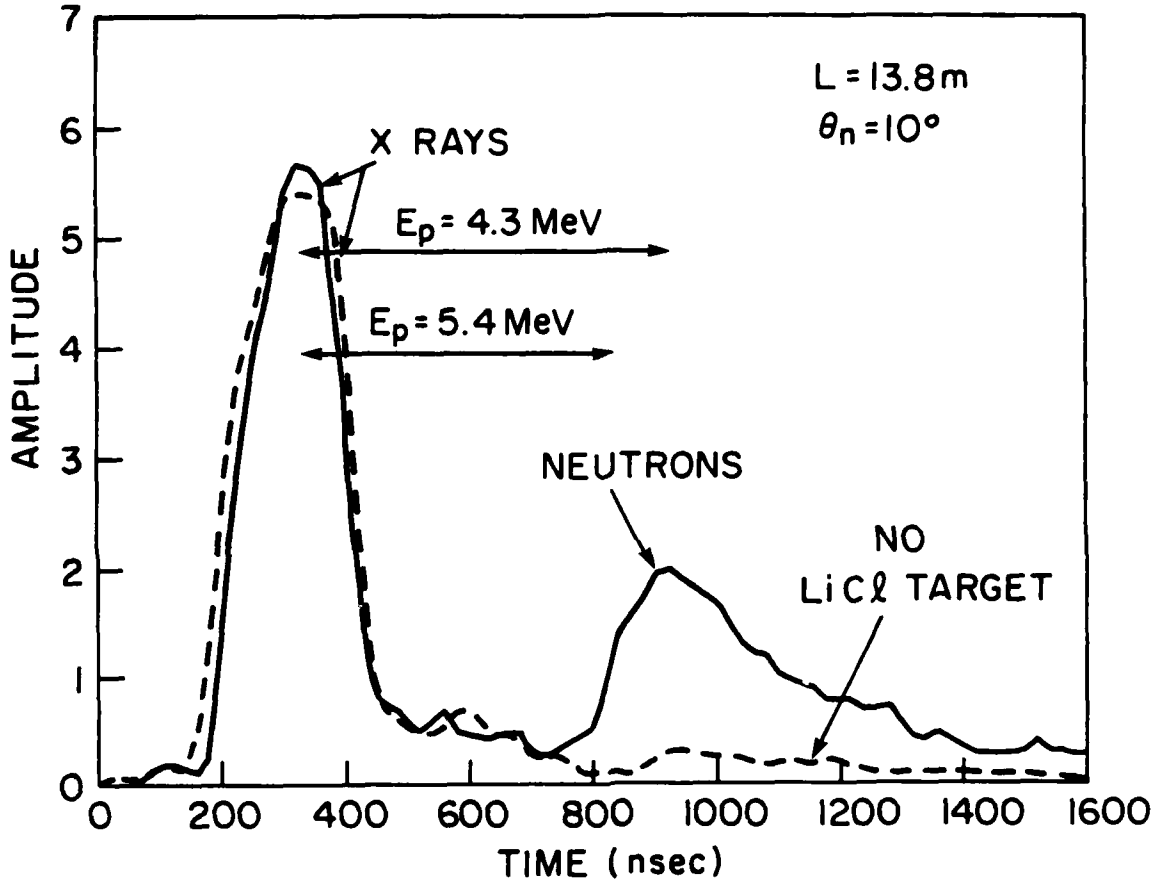

Fig. 4. Neutron TOF traces for an ion diode experiment on the Aurora generator. Neutrons from the ^{7}Li(p,n) reaction on a LiCl target (solid trace) are clearly discernible compared to a measurement without the target (dashed trace).

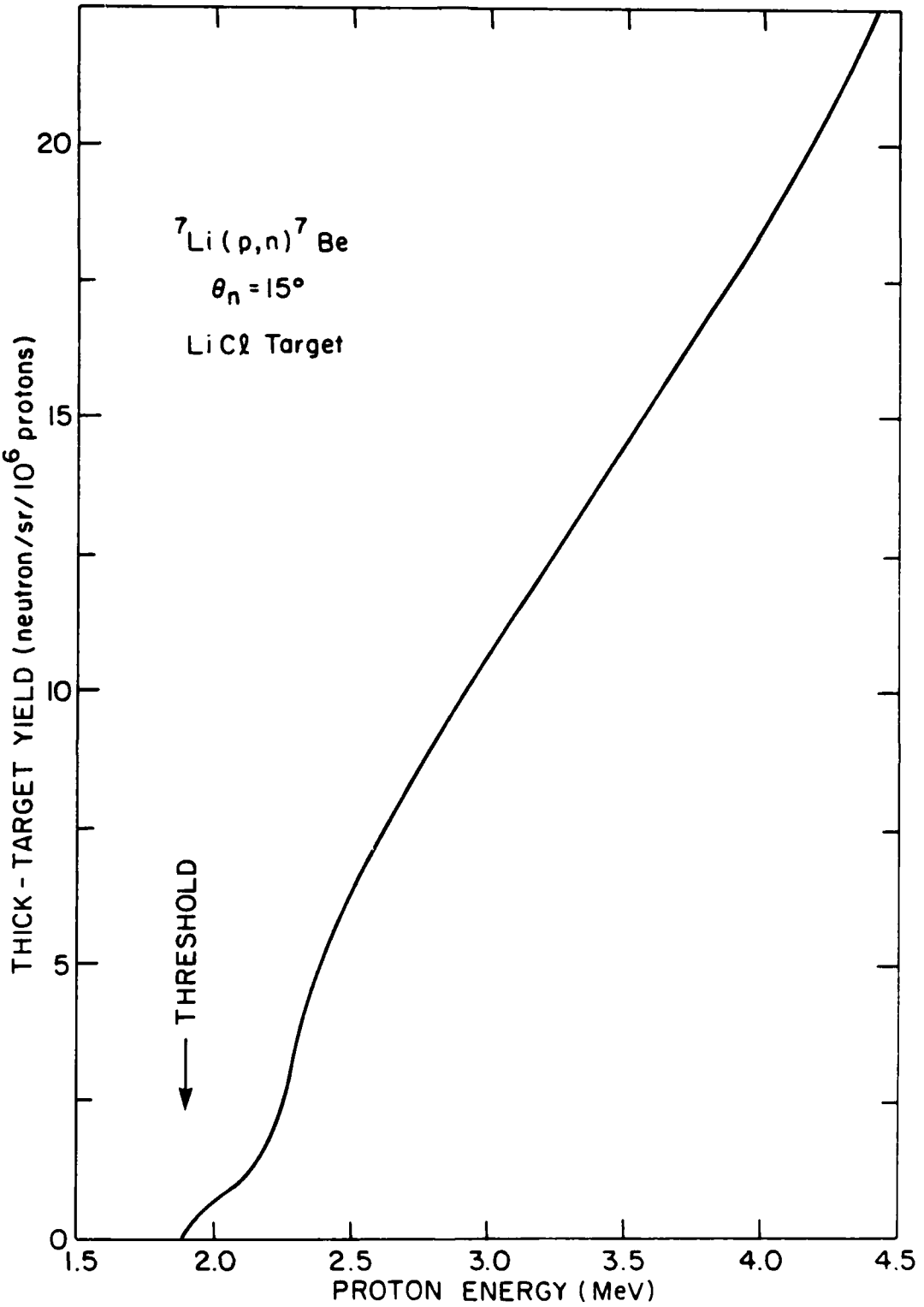

Fig. 5. Thick-target yield at 15° for the ^{7}Li(p,n)^{7}Be reaction on a LiCl target.

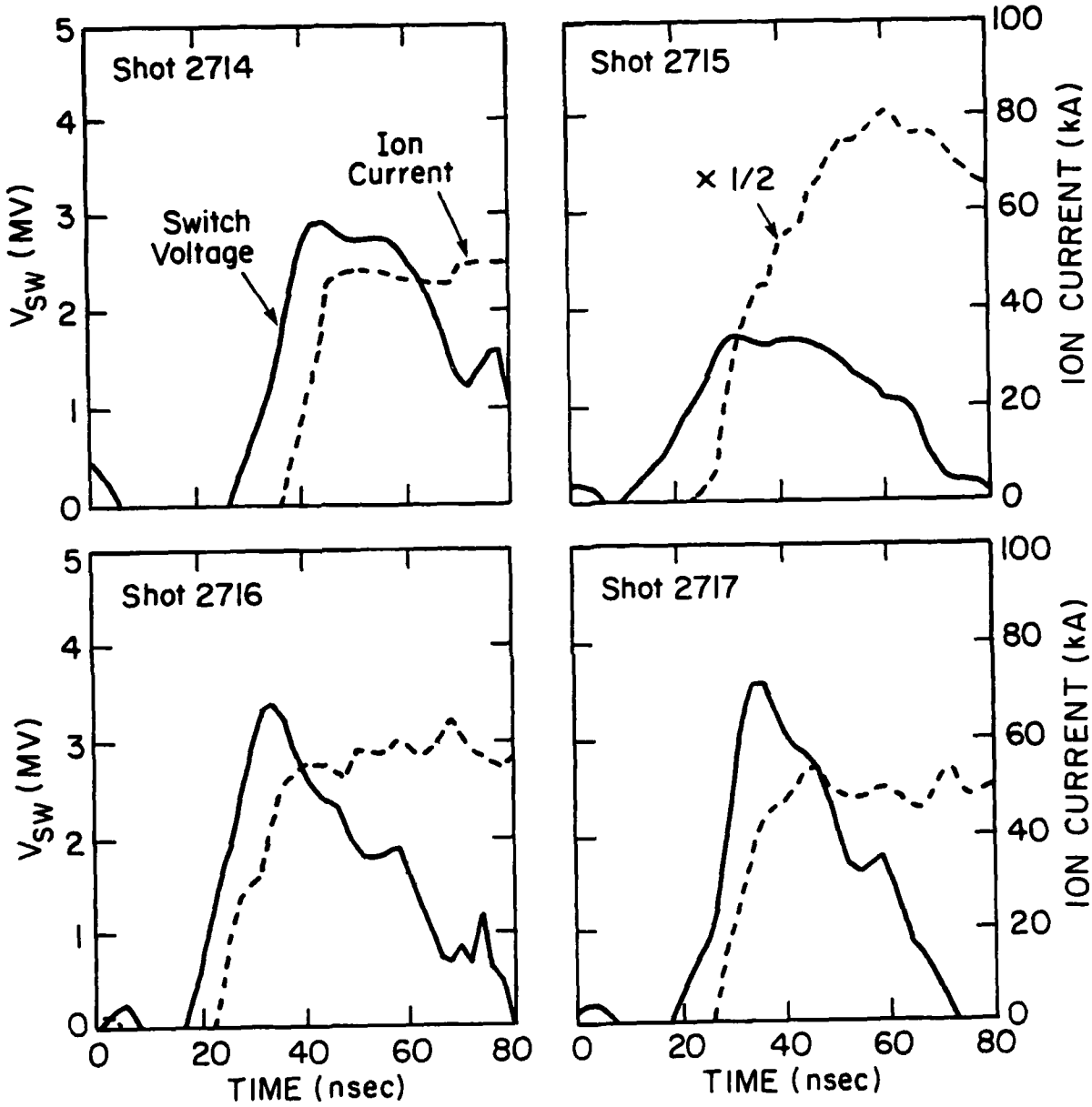

Fig. 6. Ion-current traces (dashed) and switch-voltage traces (solid) for the four Gamble II shots listed in Table II.

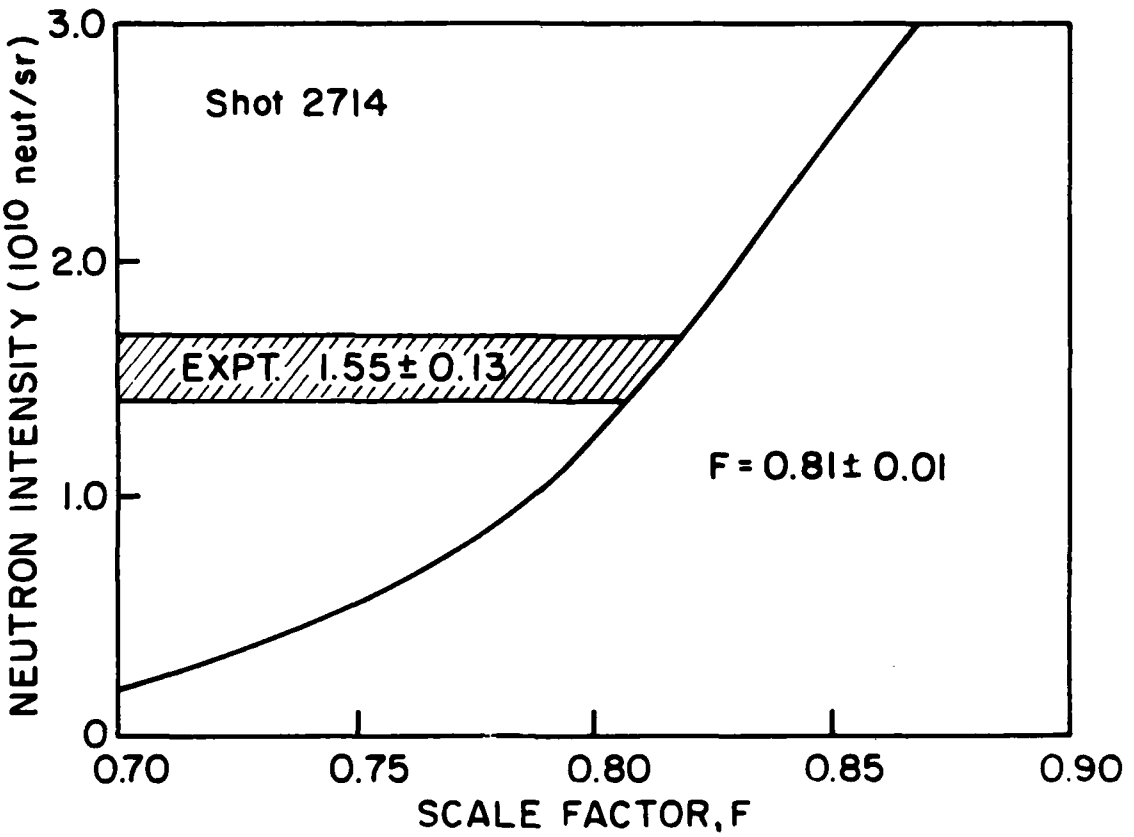

Fig. 7. Comparison of the calculated neutron intensity (solid line) as a function of the scale factor to the measured intensity for shot 2714. The measured intensity implies a scale factor of 0.81 ± 0.01.

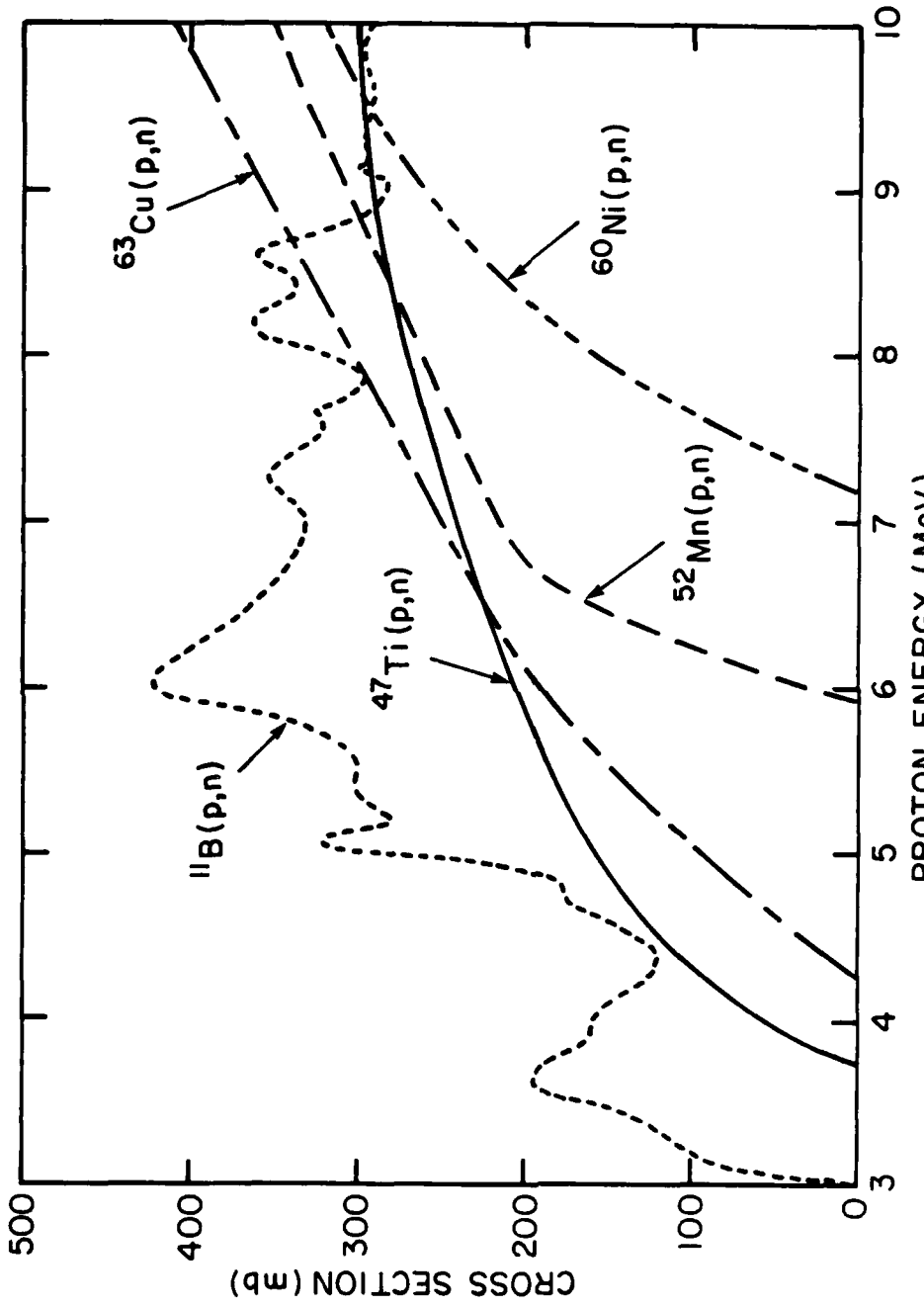

Fig. 8. Total cross sections for the (p,n) reactions listed in Table III.

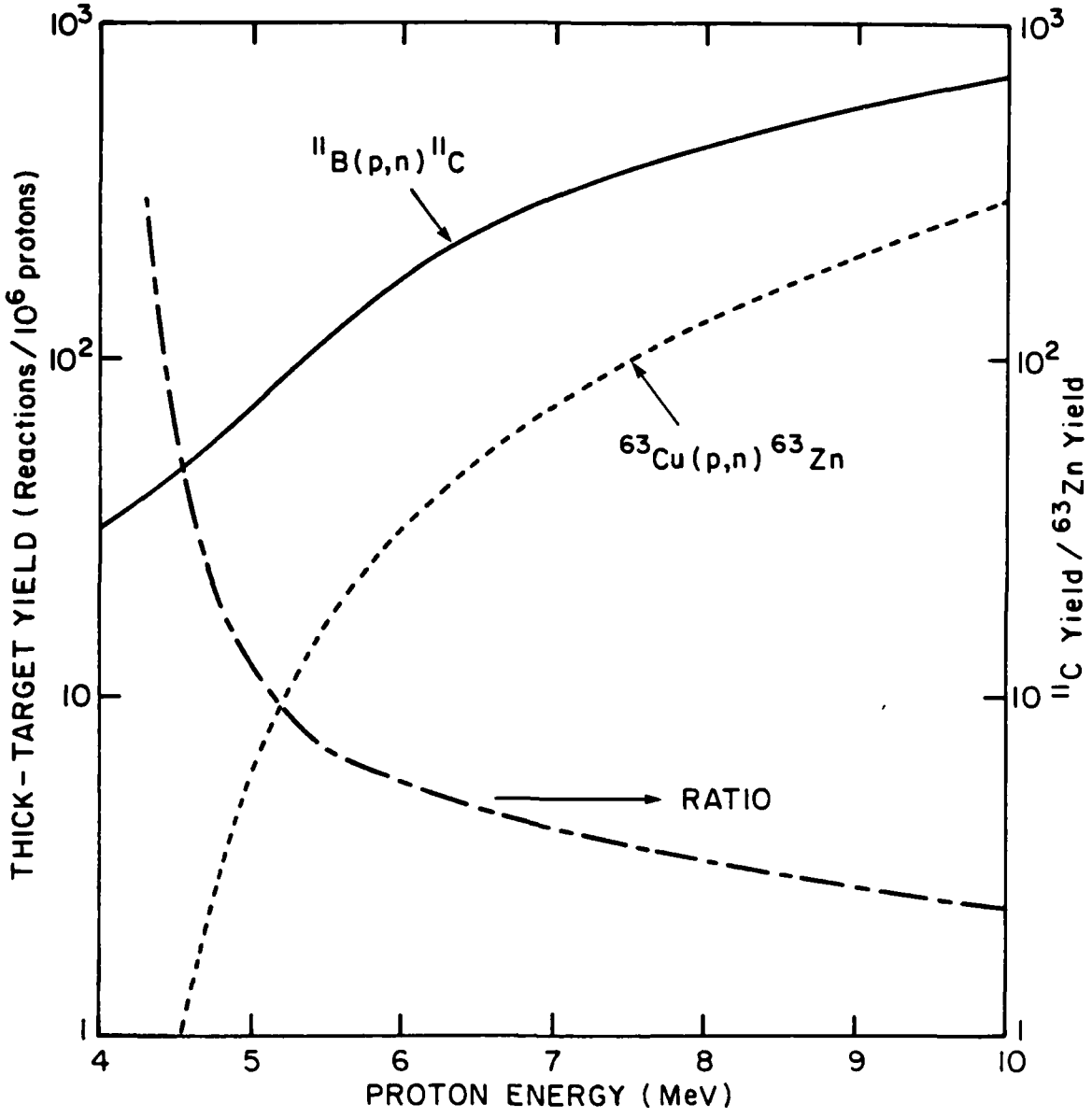

Fig. 9. Thick-target yields for the $^{11}B(p,n)^{11}C$ and $^{63}Cu(p,n)^{63}Zn$ reactions on boron nitride and copper targets, respectively. Also, the ratio of these two yields is displayed.

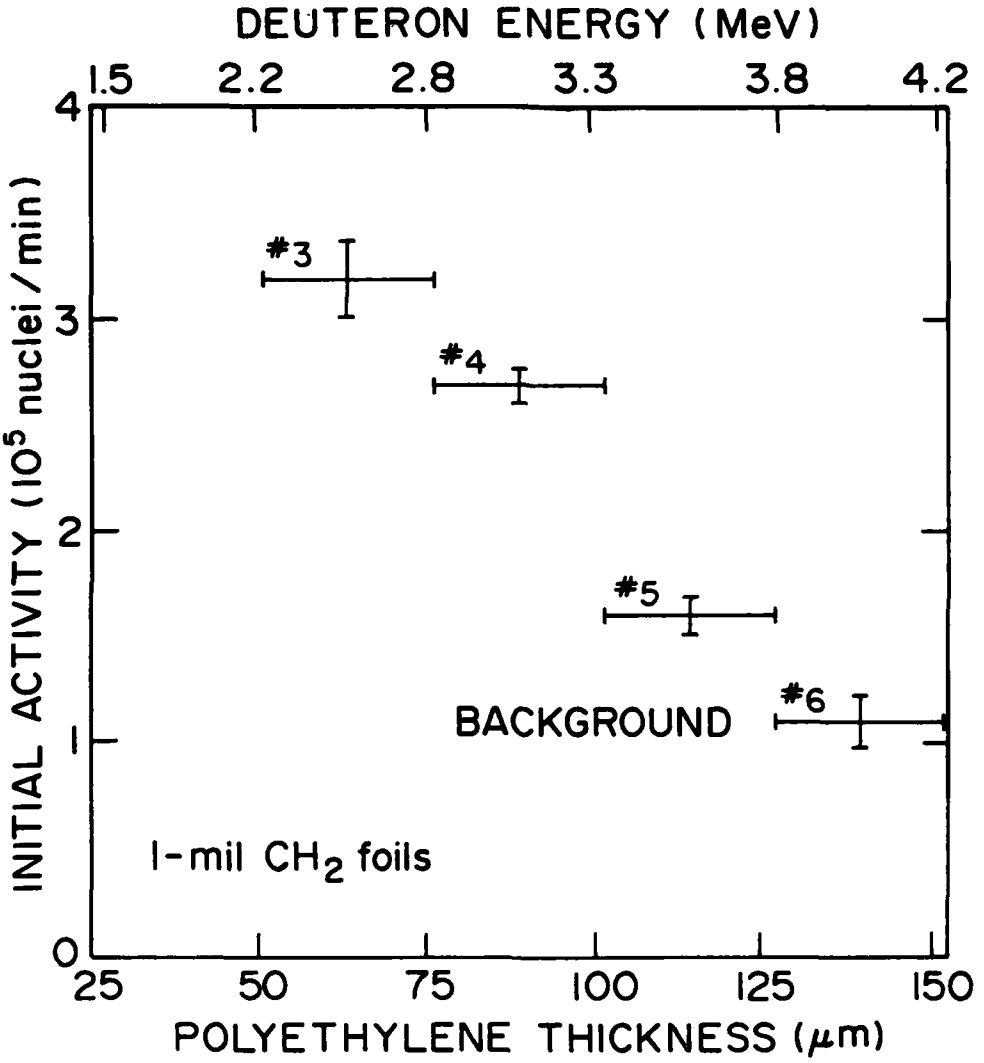

Fig. 10. Initial ^{13}N activities determined for a CH_2 foil stack as a function of depth into the stack for Shot 3013. For each foil, the vertical bar is the uncertainty in activity and the horizontal bar is the foil thickness. Foil #6 is at background level. The deuteron energy on the top scale corresponds to the range in CH_2 on the bottom scale.

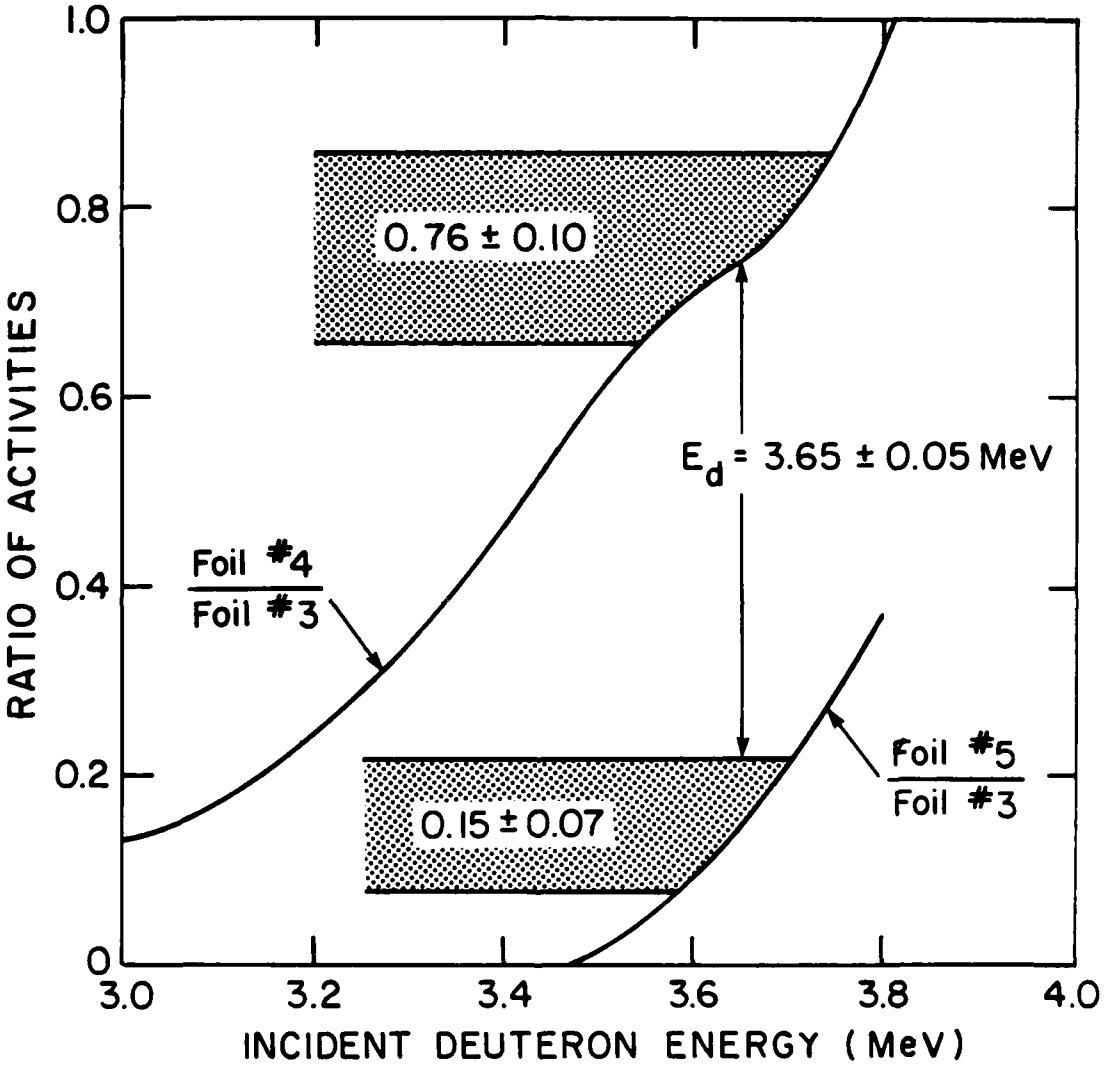

Fig. 11. Comparison of calculated and measured ratios of activities for the foil activities shown in Fig. 10. The measurements indicate a deuteron energy of 3.65 ± 0.05 MeV.

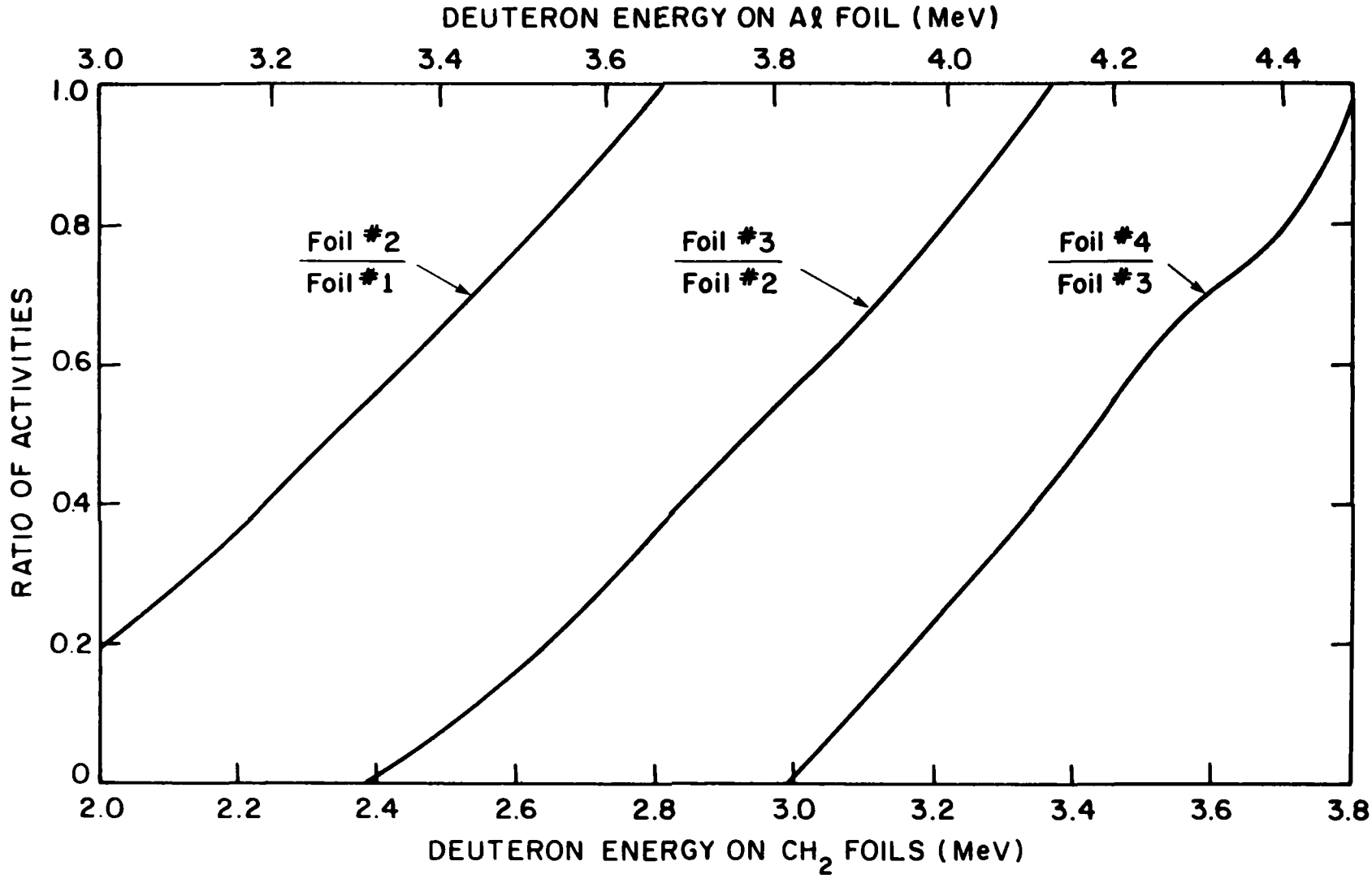

Fig. 12. Ratios of ^{13}N activities for adjacent foils in a CH_2 foil stack as a function of the deuteron energy incident on the stack. The energy on the top scale includes the energy loss in a 25-μm thick Al covering.

DISTRIBUTION FOR DOE SPONSORED WORK
4 AUGUST 1987

U.S. Department of Energy
Office of Inertial Fusion
Washington, DC 20545
Attn: S. L. Kahalas 1 copy
R. L. Schriever 1 copy

U.S. Department of Energy
Office of Classification
Washington, DC 20545
Attn: Robert T. Duff 1 copy

U.S. Department of Energy
Nevada Operations Office
P.O. Box 14100
Las Vegas, NV 89114 2 copies

U.S. Department of Energy
P.O. Box 62
Oak Ridge, TN 37830 1 copy

Cornell University
Ithaca, NY 14850
Attn: D. A. Hammer 1 copy
R. N. Sudan 1 copy

Defense Technical Information
Center Station
Duke Street
Alexandria, VA 22314
Attn: T. C. 2 copies

JAYCOR, Inc.
Spring Hill Rd.
Vienna, VA 22180-2270
Attn: B. V. Weber 1 copy
D. D. Hinshelwood 1 copy

Fusion, Inc.
Research Park Drive
P.O. Box 1567
Arbor, MI 48106
Attn: A. A. Glass 1 copy

Berkeley Laboratory
Berkely, CA 94720
Attn: D. Keefe 1 copy

Lawrence Livermore National Laboratory
P.O. Box 808
Livermore, CA 94550
Attn: R. Batzel/J. Kahn, L-1 1 copy
J. Emmett, 1-488 1 copy
W. Krupke, L-488 1 copy
E. Storm, L-481 1 copy
J. Lindl, L-477 1 copy

Los Alamos Scientific Laboratory
P.O. Box 1663
Los Alamos, NM 87545
Attn: S. D. Rockwood, ICF Prog. Mgr.
DAD/IF M/S 527 1 copy

Naval Research Laboratory
Attn: Code/Name

2628	TID Dist	22 copies
1000	T. Coffey	1 copy
4000	W. Ellis	1 copy
4040	J. Boris	1 copy
4700	S. L. Ossakow	26 copies
4701	I. Vitkovitsky	1 copy
4710	C. Kapetanakos	1 copy
4720	J. Davis	1 copy
4730	S. Bodner	1 copy
4740	W. Manheimer	1 copy
4760	B. Robson	1 copy
4770	G. Cooperstein	10 copies
4770.1	F. Young	1 copy
4771	P. Ottinger	1 copy
4771	J. Neri	1 copy
4771	J. Grossmann	1 copy
4770.1	D. Mosher	1 copy
4773	S. Stephanakis	1 copy
4790	D. Colombant	1 copy
4790	H. Haber	1 copy
4790	M. Lampe	1 copy
6682	D. Nagel	1 copy

Sandia National Laboratories
P.O. Box 5800
Albuquerque, NM 87185
Attn: J. Vandevender/1200 1 copy
D. L. Cook/1250 5 copy

University of Rochester
250 East River Road
Rochester, NY 14623
Attn: J. Eastman 1 copy

Code 1220 1 copy

Records 1 copy

END

3-88

DTIC